



Cite this: *Org. Biomol. Chem.*, 2015, **13**, 4714

Synthesis, antitumor activity, and mechanism of action of 6-acrylic phenethyl ester-2-pyrone derivatives†

Sai Fang,^{‡a} Lei Chen,^{‡a} Miao Yu,^a Bao Cheng,^a Yongsheng Lin,^a Susan L. Morris-Natschke,^b Kuo-Hsiung Lee,^{b,c} Qiong Gu^{*a,b} and Jun Xu^{*a}

Based on the scaffolds of caffeic acid phenethyl ester (CAPE) as well as bioactive lactone-containing compounds, 6-acrylic phenethyl ester-2-pyrone derivatives were synthesized and evaluated against five tumor cell lines (HeLa, C6, MCF-7, A549, and HSC-2). Most of the new derivatives exhibited moderate to potent cytotoxic activity. Moreover, HeLa cell lines showed higher sensitivity to these compounds. In particular, compound **5o** showed potent cytotoxic activity ($IC_{50} = 0.50\text{--}3.45\ \mu\text{M}$) against the five cell lines. Further investigation on the mechanism of action showed that **5o** induced apoptosis, arrested the cell cycle at G2/M phases in HeLa cells, and inhibited migration through disruption of the actin cytoskeleton. In addition, ADMET properties were also calculated *in silico*, and compound **5o** showed good ADMET properties with good absorption, low hepatotoxicity, and good solubility, and thus, could easily be bound to carrier proteins, without inhibition of CYP2D6. A structure–activity relationship (SAR) analysis indicated that compounds with *ortho*-substitution on the benzene ring exhibited obviously increased cytotoxic potency. This study indicated that compound **5o** is a promising compound as an antitumor agent.

Received 4th January 2015,

Accepted 10th March 2015

DOI: 10.1039/c5ob00007f

www.rsc.org/obc

Introduction

Cancer is a major public health problem in many parts of the world, accounting for 23% of all deaths and was second only to heart diseases in 2014.¹ Among various cancers, lung cancer is the most common cause of deaths, accounting for more than one-quarter of all cancer deaths in men and women. Other cancers, such as prostate in men and breast in women, are also very common causes of deaths from cancer.²

Caffeic acid phenethyl ester (CAPE) (Fig. 1) is the main constituent of propolis, a resinous substance used in folk medicine for treating various ailments. CAPE was widely reported to possess anti-inflammatory, antibacterial, antiviral, and antitumor activities.³ Moreover, CAPE selectively inhibited proliferation of several types of carcinoma cell lines, but showed almost no toxic effects on normal peripheral blood cells or

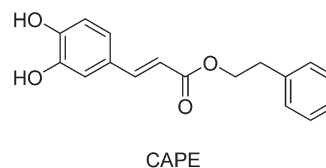


Fig. 1 Chemical structure of CAPE.

normal hepatocytes. Some CAPE derivatives showed potent activity against lung cancer, prostate cancer, melanoma,⁴ uterine corpus cancer, breast cancer,⁵ glioma,⁶ leukemia,⁷ and oral cancer.⁸ Omene and co-authors⁹ also demonstrated that CAPE induced cell cycle arrest and apoptosis and inhibited angiogenesis.

In our continuing studies to modify antitumor natural products for increased potency, we aimed to determine whether the catechol moiety is essential for the cytotoxic activity of CAPE and its related derivatives. Our plan was to change the catechol ring to a lactone ring, specifically a 4-methoxy-2H-pyran-2-one. Lactone ring systems are found in many bioactive natural products obtained from plants, animals, marine organisms, bacteria, and insects,¹⁰ including those that exhibit various pharmacological activities, such as HIV protease inhibitory,¹¹ anticonvulsant,¹² antimicrobial,¹³ antitumor,^{14,15} and other effects. Examples include styryl-2-pyrone,¹⁶ isorumbin,¹⁷ bufadienolide,¹⁸ neo-tanshinlactone,¹⁹ wortmannin,²⁰

^aResearch Center for Drug Discovery, School of Pharmaceutical Sciences, Sun Yat-sen University, Guangzhou 510006, People's Republic of China.

E-mail: junxu@biochemomes.com, guqiong@mail.sysu.edu.cn

^bNatural Products Research Laboratories, UNC Eshelman School of Pharmacy, University of North Carolina, Chapel Hill, North Carolina 27599, USA

^cChinese Medicine Research and Development Center, China Medical University and Hospital, Taichung, Taiwan

†Electronic supplementary information (ESI) available. See DOI: 10.1039/c5ob00007f

‡These authors contributed equally to this work.

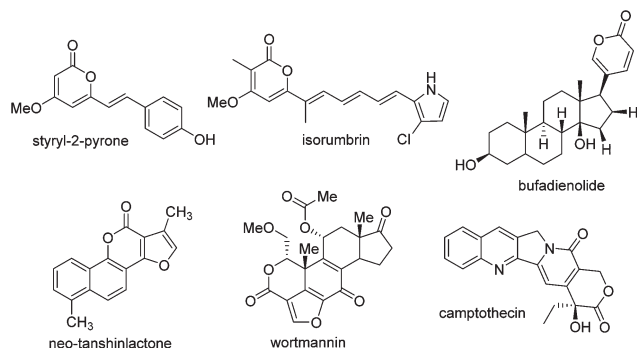


Fig. 2 Chemical structures of several natural products with lactone rings.

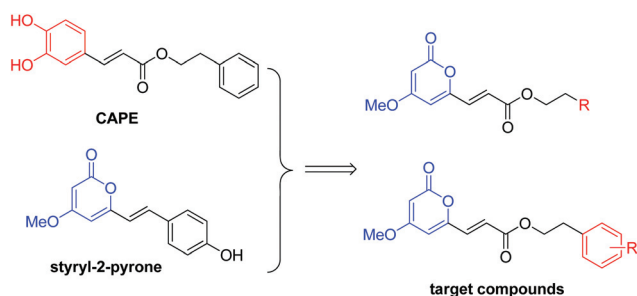


Fig. 3 Design for the 6-acrylic phenethyl ester-2-pyrone derivatives.

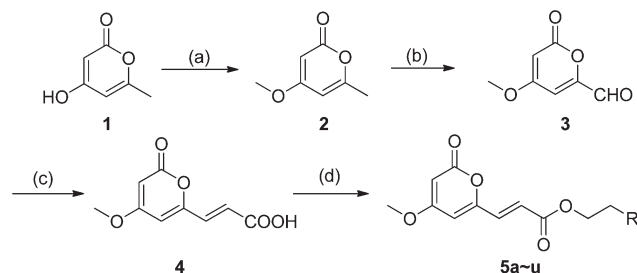
and camptothecin,²¹ as shown in Fig. 2. Based on numerous modification studies, such as those performed on camptothecin and its derivatives, a lactone ring can be an important pharmacophore in anticancer drugs.²²

Therefore, based on the antitumor activity of CAPE and various lactone-containing compounds, we combined both CAPE and styryl-2-pyrone scaffolds as chemical starting points to design chemically modified CAPE analogues, which contain variously substituted acrylic phenethyl esters and a 4-methoxy-2-pyrone moiety (Fig. 3). Subsequently, 21 new CAPE derivatives were synthesized and evaluated against five tumor cell lines. Preliminary structure–activity relationship (SAR) correlations were also obtained, and the antitumor mechanism of action was also investigated.

Results and discussion

Chemistry

The series-5 target compounds were synthesized according to the approaches illustrated in Scheme 1. Compounds 2 and 3 were synthesized according to literature methods.²³ Initially, compound 2 was obtained by methylation of commercially obtained 4-hydroxy-6-methyl-2H-pyran-2-one (1). Then, the methyl group at C-6 of 2 was oxidized with selenium dioxide in 1,4-dioxane in a sealed tube at 160 °C to yield 3. The intermediate (*E*)-3-(4-methoxy-2-oxo-2H-pyran-6-yl)acrylic acid (4)



Scheme 1 Synthesis of 5a–u. Reagents and conditions: (a) Me_2SO_4 , K_2CO_3 , acetone, r.t., 16 h, 84%; (b) SeO_2 , dioxane, 160 °C, 4 h, 91%; (c) $\text{CH}_2(\text{COOH})_2$, pyridine, piperidine, reflux, 3 h, 47%; (d) phenethyl alcohols or heterocyclic EtOHs, EDC·HCl, DMAP, CH_2Cl_2 , r.t., overnight, 49%–71%.

was obtained in 47% yield through a Knoevenagel condensation reaction with the reaction temperature set at 110 °C. As we know, the general condition of the Knoevenagel condensation reaction to afford cinnamic acid derivatives is with piperidine as the base, pyridine as the solvent, and the reaction temperature is at room temperature. Since the lactone ring in the target compound was not stable in strong basic solution, we explored several bases, such as K_2CO_3 , Et_3N , EtONa , and piperidine. As a result, piperidine was found to be the best. To discover the best solvent, we explored methanol, ethanol, and pyridine. Pyridine is a commonly used solvent for Knoevenagel condensation, and we found that it was also the best solvent to afford our desired compound 4. The reaction temperature was also optimized. Room temperature, 60 °C, and reflux temperature were investigated, and we found that the reflux reaction temperature was the best. So we chose piperidine as the base, pyridine as the solvent, and the reaction temperature was at reflux. Finally, our desired series-5 compounds were prepared from 4 through an esterification reaction using 1-ethyl-3-(3-dimethylaminopropyl)carbodiimide hydrochloride (EDC·HCl) as a condensing reagent. The obtained yields were varied from 49% to 71%.

Antitumor activity against five human cancer cell lines

To evaluate the effects of 5-derivatives on the growth of human cancer cells, the growth inhibitory potential was evaluated using a MTT assay in five human cancer cells. Initially, 12 compounds (5a–l) were screened at 20 μM . Only compounds 5b and 5e exhibited significant *in vitro* antitumor activity (greater than 50% growth inhibition) against the tested human cancer cell lines at this concentration. Table 1 lists the IC_{50} values for the active compounds. Interestingly, both 5b and 5e were substituted at C-2 of the benzene ring, while the inactive compounds (5a, 5c, 5e, 5f, and 5g) were substituted at the C-3 or C-4 position or contained a heterocyclic rather than a benzene ring (5h–l). While substitution at C-2 sharply affected the antitumor activity, both chlorine and methyl groups had similar impacts (compare 5b vs. 5e). Moreover, both new lactone-containing CAPE-derivatives were more

Table 1 *In vitro* cytotoxicity data for **5a–l** against five human tumor cell lines

Compound	Structure	IC ₅₀ (μM)				
		MCF-7	C6	HSC-2	HeLa	A549
CAPE		NA ^b	NA ^b	NA ^b	NA ^b	NA ^b
5a		— ^a	— ^a	— ^a	— ^a	— ^a
5b		6.56	NA ^b	1.24	1.14	NA ^b
5c		— ^a	— ^a	— ^a	— ^a	— ^a
5d		— ^a	— ^a	— ^a	— ^a	— ^a
5e		3.13	6.77	0.92	2.31	10.3
5f		— ^a	— ^a	— ^a	— ^a	— ^a
5g		NA ^b	— ^a	— ^a	8.27	— ^a
5h		— ^a	— ^a	— ^a	— ^a	— ^a
5i		— ^a	— ^a	— ^a	— ^a	— ^a
5j		— ^a	— ^a	— ^a	— ^a	— ^a
5k		— ^a	— ^a	— ^a	— ^a	— ^a
5l		— ^a	— ^a	— ^a	— ^a	— ^a

^a Growth inhibition did not reach 50% at 20 μM. ^b NA = IC₅₀ > 10 μM.

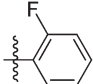
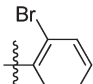
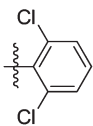
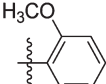
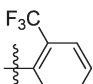
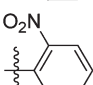
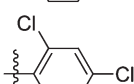
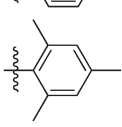
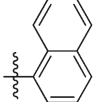
active than CAPE, especially against MCF-7, HSC-2, and HeLa cancer cell lines.

On the basis of the preliminary results, nine additional **5**-derivatives were synthesized to more fully evaluate the effects of substituents at C-2 on the cytotoxicity. Compounds **5m–u** contained –F, –Br, –OCH₃, –CF₃, and –NO₂ substituents, as well as multiply substituted phenyl rings or a naphthyl ring. The assay results are shown in Table 2. Compounds with a 2-F or 2-NO₂ group (**5m** and **5r**, respectively) were inactive against all cancer cell lines, whereas the derivative with a 2-Br group (**5n**) was active against four cell lines. These results demonstrated that stronger electron-withdrawing inductive effects decreased the antitumor activity. Compounds with a 2-methoxy (**5p**) or 2-trifluoromethyl (**5q**) group were active only against the HeLa cell lines, which appeared to have the greatest sensitivity to this compound class. Among the compounds

with multiple substituents on the phenyl ring, the 2,4,6-trimethylated compound (**5t**) showed significant activity against the MCF-7, HSC-2, and HeLa cell lines. A comparison of **5o**, **5b**, and **5s** indicated that the former compound with a 2,6-disubstituted benzene ring displayed better activity against all five tested cell lines than the latter compounds with 2- or 2,4-substitution. Finally, when the benzene ring was changed to a naphthalene ring (**5u**), no cytotoxicity was observed. This finding indicated that greater steric bulk could lead to decreased antitumor activity.

Among all 21 compounds, **5o** showed most potent activity against the five tested human tumor cell lines (IC₅₀: 2.61, 3.45, 1.19, 0.50, and 1.15 μM). Moreover, the lowest IC₅₀ value for **5o** (0.50 μM) was obtained in HeLa cells compared with the other cell lines. The effect of **5o** on cell proliferation in HeLa cell lines was also assayed as shown in Fig. 4. Cells treated with **5o**

Table 2 *In vitro* cytotoxicity data for 5m–u against five human tumor cell lines

Compound	Structure	IC ₅₀ (μM)				
		MCF-7	C6	HSC-2	HeLa	A549
5m		— ^a	— ^a	— ^a	— ^a	— ^a
5n		5.01	NA ^b	2.62	1.47	7.03
5o		2.61	3.45	1.19	0.50	1.15
5p		NA ^b	NA ^b	NA ^b	5.63	NA ^b
5q		NA ^b	— ^a	— ^a	9.13	— ^a
5r		— ^a	— ^a	— ^a	— ^a	— ^a
5s		NA ^b	NA ^b	9.45	6.26	NA ^b
5t		7.99	NA ^b	3.52	1.49	NA ^b
5u		— ^a	— ^a	— ^a	— ^a	— ^a

^a Growth inhibition did not reach 50% at 20 μM. ^b NA = IC₅₀ > 10 μM.

(0.5 and 1 μM) displayed morphological changes and showed distinctly rounded shapes compared with the control cells (Fig. 4B). This result prompted us to study the mechanism of action of 5o in HeLa cell lines.

Cell cycle effects of 5o

Based on previous investigation, cell proliferation is associated with regulation of three phases (G0/G1, S, and G2/M) of the cell cycle. To investigate if growth inhibition induced by 5o was associated with regulation of the cell cycle, cycle distribution of HeLa cells with or without 5o treatment was analyzed by flow cytometry. As shown in Fig. 5B, the untreated group of HeLa cells had a low proportion of cells in G2/M (39.17%), while the experimental groups treated with 5o (0.5, 1, and 2 μM) for 24 h showed increased proportions of G2/M phase cells (51.62%, 68.45%, and 73.82%, respectively). These

results suggested that 5o inhibited cell growth by arresting the cell-cycle at the G2/M phase in a concentration-dependent manner. Furthermore, sub-G0/G1 phase cells were observed after 5o exposure (Fig. 5A), which indicated that 5o induced apoptosis of HeLa cells.

Cell cycle progression is driven by cyclins and cyclin-dependent kinases (Cdks).²⁴ Generally, Cdc25c, Cdc2 kinases and CyclinB1 are primarily activated at the G2/M phase.²⁵ The cell cycle transition from the G2 phase to the M phase is controlled by Cdc2/CyclinB1 kinase complex activity, which is activated by Cdc25C. Cdc25C activity is a rate-limiting process for G2/M phase transition.^{24b} Subsequent experiments were performed to analyze changes in the expression of key G2/M checkpoint regulatory proteins using western blot. As shown in Fig. 5D, cells treated with 5o for 48 h had decreased levels of CyclinB1, mitotic cyclin-dependent kinase Cdc2, and mitotic Cdc25C in a dose-dependent manner. These results are consistent with

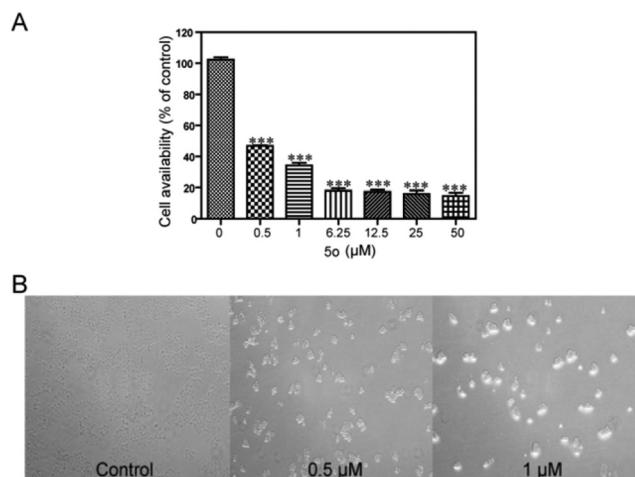


Fig. 4 The inhibitory effects of **5o** on HeLa cell growth. (A) Cells were treated or untreated with increasing concentrations (0.5–50 μM) of **5o** for 48 h. (B) Effects on cell morphology after treatment with **5o** (0.5, 1 μM) under a phase contrast microscope at 100 \times magnification. ***Significant difference compared to the control group ($P < 0.001$).

G2/M arrest and demonstrated that **5o** inhibited the proliferation of HeLa cells by G2/M-phase arrest.

Induction of apoptosis by **5o** in HeLa cell lines

As a natural process of programmed cell death (PCD), apoptosis plays an important role in cell clearance. Based on current studies, extensive apoptosis is observed in regressing tumor cells and also in those cells treated with chemotherapeutic agents.²⁶ There is a lot of evidence to show that apoptosis is the most crucial and renowned mechanism for clearance of tumor cells.²⁷ Apoptosis tolerance may result in treatment resistance.²⁸ In the previous analysis of the **5o**'s effect on the cell cycle, a sub-G0/G1 peak was observed (Fig. 5A). In order to confirm that the sub-G0/G1 peak was caused by apoptosis rather than by cell debris, quantitative apoptotic analysis was performed by using an Annexin V-FITC/PI Apoptosis Detection Kit (Becton Dickinson, USA). As shown in Fig. 6A, in HeLa cells treated with **5o** at indicated concentrations for 24 h, the percentages of early/late apoptotic cells were 7.52%/1.66%, 7.18%/2.25%, and 10.2%/2.50% compared to control (1.05%/0%). These results indicated that **5o** induced HeLa cell apoptosis, especially early apoptosis.

To further confirm that **5o** induced apoptosis, the expressions of key apoptosis-related proteins, such as caspase-3 and PARP, were detected by western blot assay. Caspase proteins play a central role in the execution-phase of cell apoptosis. Among caspase proteins, caspase-3 is a critical executioner of apoptosis. Caspase-3 can be activated both by extrinsic (death ligand) and intrinsic (mitochondrial) apoptotic pathways.²⁹ Caspase-3 activation is dominant and reflected in the cleavage of PARP, which is a substrate of caspase-3.³⁰ Cleavage of PARP results in DNA repair inhibition and DNA degradation. As shown in Fig. 6B, treatment with **5o** for 48 h signifi-

cantly increased the level of cleaved caspase-3 (active form of caspase-3) in a dose-dependent manner compared with the control group. At the same time, total full-length PARP (116 kDa) was cleaved into a large fragment (89 kDa), and cleaved PARP also increased remarkably in a dose-dependent manner. These findings corresponded with the activation of caspase-3 and the data demonstrated that **5o** induced HeLa cell apoptosis through activation of the caspase-mediated pathway.

5o Induced morphological changes by actin cytoskeleton disruption

As shown in Fig. 4B, significant changes in cell morphology were observed. HeLa cells treated with **5o** (0.5 and 1 μM) for 24 h exhibited a distinctly round shape and detachment compared to the untreated cells. Cell morphology and adhesion are usually associated with the actin cytoskeleton.³¹ Therefore, immunofluorescence microscopy was used to explore the effect of **5o** on the actin cytoskeleton. In the control group, actin was diffusely distributed, whereas in the **5o**-treated group (0.5 μM), actin was locally clustered. When HeLa cells were treated with 1 μM of **5o**, actin aggregation was enhanced and actin disruption was also generated (Fig. 7). In addition, apoptotic bodies (denoted by red mark), which are consistent with apoptosis-induced conclusion, were observed in HeLa cells treated with 1 μM of **5o**. These results suggested that **5o** induced actin aggregation and further disrupted the actin cytoskeleton. Because a disequilibrium of the actin dynamics between G-actin and F-actin can result in actin aggregation and influence cell shape and cell adhesion,³² we speculated that **5o** induced actin aggregation and actin cytoskeleton disruption through disturbing the actin dynamic equilibrium. Actin dynamics is essential for cell division. G2/M-phase blockage of **5o** may also contribute to the abnormal actin dynamics, but the detailed mechanism should be further confirmed.

Inhibition of cell migration and invasion

Malignant tumor invasion and metastasis have been hot and difficult research topics in oncology. Tumor cells use their intrinsic migratory ability to invade adjacent tissues and the vasculature and, ultimately, to metastasize.³³ Migration and invasion of cancer cells are dependent on the actin cytoskeleton,³⁴ which are driven by the polymerization of actin within two distinct structures, lamellipodia and filopodia, and attachment to the extracellular matrix through actin-rich adhesive structures.³⁵ In previous confocal assays, we observed that **5o** disturbed the actin dynamics and disrupted the actin cytoskeleton. Subsequently, we conducted invasion and migration assays to explore whether **5o** influenced the migration and invasion abilities of HeLa cells. In Fig. 8, HeLa cells with or without treatment of different doses of **5o** were stained by crystal violet. As shown in Fig. 8, in a Matrigel-coated (for migration ability) or -noncoated (for invasion ability) Transwell assay, the numbers of HeLa cells passing through the filter were significantly decreased in response to increasing concentrations of **5o**. These results demonstrated that **5o** could mark-

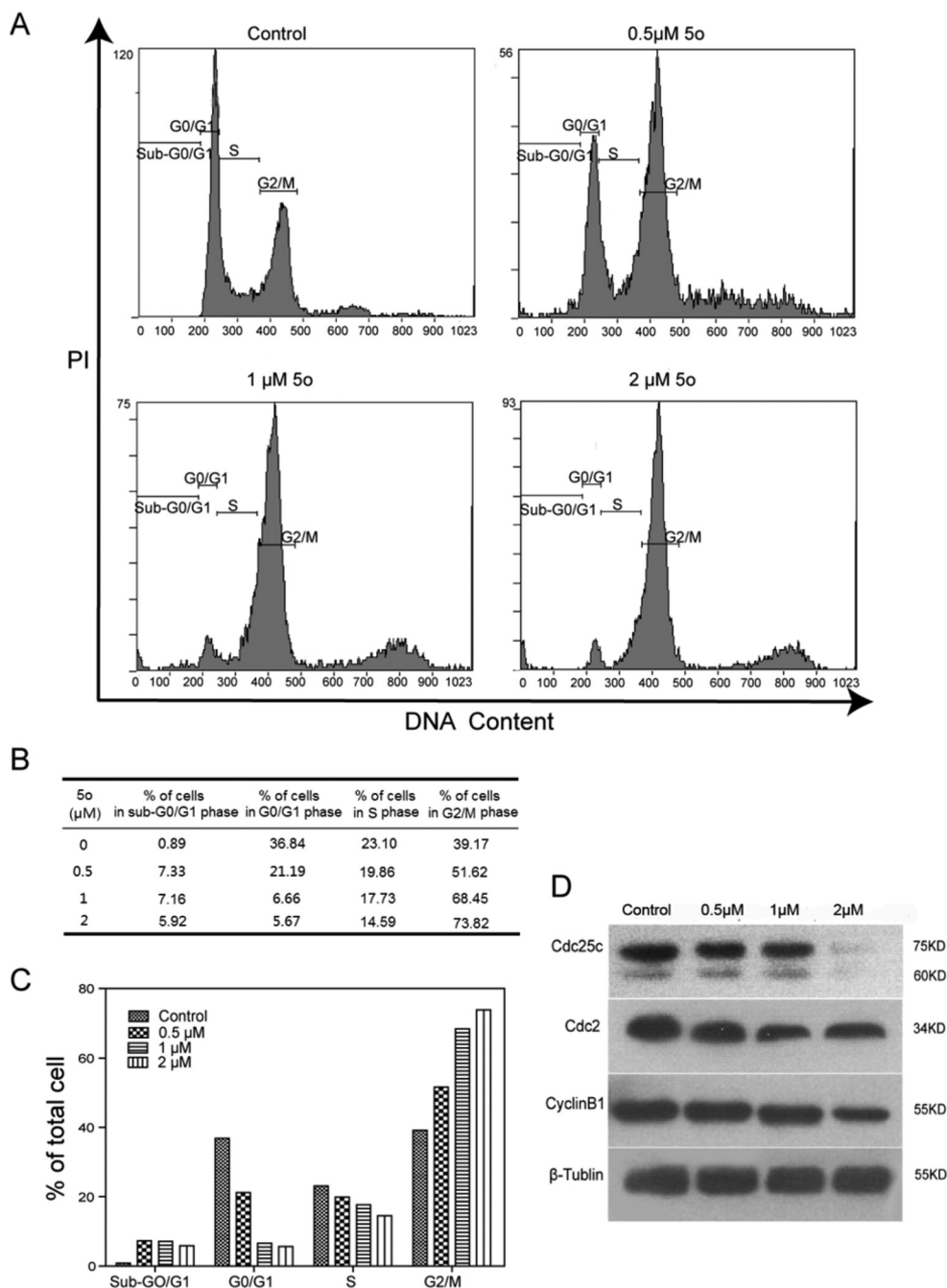


Fig. 5 **5o** Induced G2/M arrest by modulating the expression of cell cycle-related proteins in the G2/M phase. (A) Cells were treated with **5o** (0, 0.5, 1 and 2 μ M) for 24 h, and stained with PI and RNase A, then analyzed by flow cytometry to determine sub-G1 and cell-cycle phases. (B) Distribution of cells (%) treated with **5o** in cell-cycle phases (sub-G0/G1, G0/G1, S, and G2/M). (C) The histogram analysis of (B). (D) After **5o** (0, 0.5, 1 and 2 μ M) treatment for 48 h, G2/M phase related protein (cyclin B1, Cdc2, and Cdc25C) levels were detected by western blot.

edly inhibit both migration and invasion abilities of HeLa cells.

Preliminary ADMET study

To investigate the drug-like profiles of the synthesized compounds, we subjected several 5-series compounds for preliminary ADMET prediction (Table 3). Improved blood–brain

barrier (BBB) penetration and decreased liver toxicity were calculated for **5o** in comparison with CAPE. In addition, calculations indicated that **5o** had good absorption and solubility and could easily be bound to carrier proteins in the blood, while showing no inhibition of CYP2D6. However, **5o** should still be evaluated experimentally and further optimized regarding its pharmacokinetics properties.

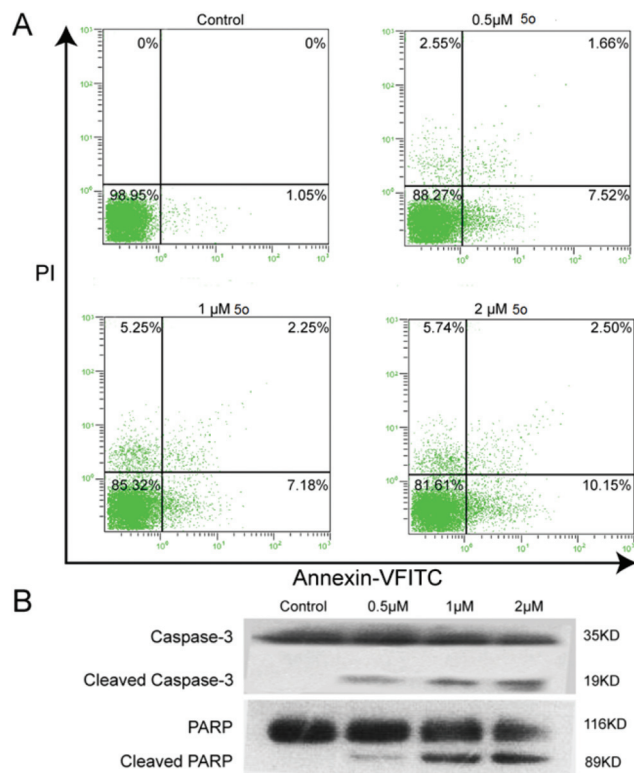


Fig. 6 **5o** Induces apoptosis *via* a caspase-dependent pathway. (A) HeLa cell lines were treated with **5o** (0, 0.5, 1 and 2 μM) for 24 h, and stained with Annexin-V FITC/PI, then analyzed by flow cytometry to evaluate apoptosis. (B) Western blot analysis of apoptosis-related protein (caspase-3 and PARP) levels in HeLa cell lines exposed to **5o** (0, 0.5, 1 and 2 μM) for 48 h.

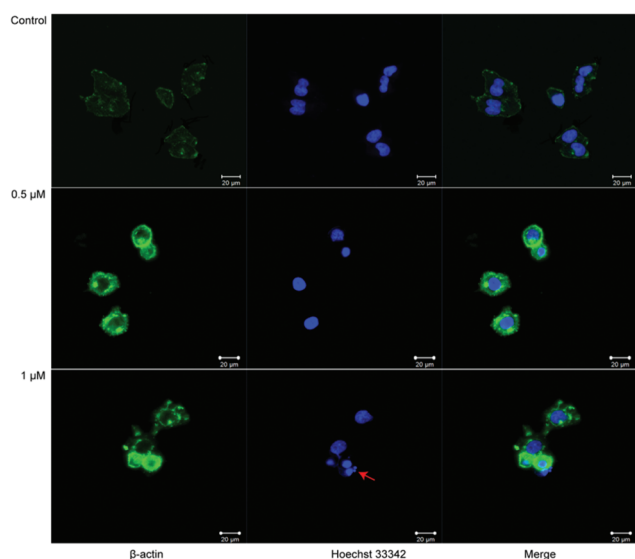


Fig. 7 Immunofluorescence microscopy analysis of the actin cytoskeleton in HeLa cell lines with **5o** treatment. Cells were either untreated or treated with **5o** (0.5, 1 μM) for 24 h, and then immunofluorescence assay was conducted as described in the Experimental section. The β-actin (green) was revealed by single-immunofluorescence staining. Nuclei (blue) were stained by using Hoechst 33342. Scale bar, 20 μM.

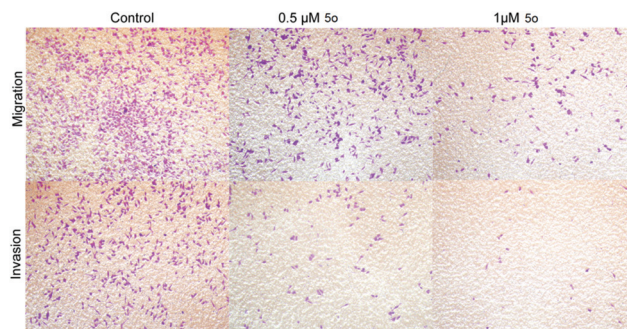


Fig. 8 Compound **5o** inhibited HeLa cell line migration and invasion in a Transwell assay. Invasion potential of HeLa cells passing through Matrigel-coated Transwell after treatment with the indicated concentration of **5o** for 24 h. Migration potential is without Matrigel. These images show the number of HeLa cells passing through the filter with/without Matrigel. As the **5o** dose increased, the number of cells on the undersurface of the filter decreased.

Conclusion

In summary, the acrylic phenethyl ester portion of CAPE was combined with the 4-methoxy-2H-pyran-2-one of styryl-2-pyrone, and a series of 6-acrylic phenethyl ester-2-pyranone derivatives were designed and synthesized. Among the new compounds, **5o** exhibited significantly more anti-proliferation activity than CAPE against five human cancer cell lines. Particular efficacy was observed against the HeLa cell lines ($IC_{50} = 0.50 \mu M$). Flow cytometric analysis of the cell cycle demonstrated an increased percentage of G2/M phase cells in **5o**-treated cells. More importantly, **5o** induced HeLa cell apoptosis *via* a caspase-3-dependent manner. Moreover, further study indicated that **5o** influenced invasion and migration in HeLa cells by disrupting the actin cytoskeleton. In addition, based on *in silico* ADMET predictions, compound **5o** is likely to demonstrate good ADMET properties with low hepatotoxicity. These findings suggest that **5o** is a promising compound for further study to generate a clinical trial candidate for the treatment of cancer.

Experimental

Synthesis

Materials and equipment. Reagents were used without further purification unless otherwise specified. Solvents were dried and redistilled prior to use by usual methods. The 1H NMR and ^{13}C NMR spectra were recorded using TMS as the internal standard on a Bruker BioSpin GmbH spectrometer (Avance III, Switzerland) at 400 MHz and 100 MHz. Coupling constants are given in Hz. High-resolution mass spectra were obtained using a Shimadzu LCMS-IT-TOF mass spectrometer. Flash column chromatography was performed using silica gel (200–300 mesh) purchased from Qingdao Haiyang Chemical Co., Ltd or alumina from Sinopharm Chemical Reagent Co.,

Table 3 The parameters of ADMET descriptors of 5 series

Compound	BBB ^a	Absorption ^b	Solubility ^c	Hepatotoxicity ^d	CYP2D6 ^e	PPB ^f
5b	2	0	3	0	0	2
5e	2	0	3	1	0	2
5g	2	0	3	1	0	2
5n	2	0	3	1	0	2
5o	1	0	2	0	0	2
5p	2	0	3	1	0	2
5q	2	0	2	1	0	1
5s	1	0	2	1	0	2
5t	1	0	2	0	0	1
CAPE	2	0	3	1	0	2

^a BBB is blood–brain barrier penetration and predicts blood–brain penetration after oral administration. 1 (high), 2 (medium). ^b Absorption predicts human intestinal absorption (HIA) after oral administration. 0 (good). ^c Solubility predicts the solubility of each compound in water at 25 °C. 2 (low), and 3 (good). ^d Hepatotoxicity predicts potential liver toxicity of compounds. 0 (Nontoxic), 1 (toxic). ^e CYP2D6 predicts CYP2D6 enzyme inhibition using the 2D chemical structure. 0 (Non-inhibitor). ^f PPB predicts whether a compound is likely to be highly bound to carrier proteins in the blood. 1 (Binding ability >90%), 2 (binding ability >95%).

Ltd. All reactions were monitored by thin layer chromatography using silica gel.

Synthesis of 4-methoxy-6-methyl-2H-pyran-2-one (2)²³

To a suspension of K₂CO₃ (62.4 g, 452.4 mmol) in anhydrous acetone (200 mL) under nitrogen was added Me₂SO₄ (9.8 mL, 103.2 mmol). Then, the substrate 4-hydroxy-6-methyl-2H-pyran-2-one (1) (10.0 g, 79.36 mmol) was added in one portion. The reaction mixture was stirred at room temperature for 16 h. Then, the system was filtered, the obtained solid was washed with acetone, and the solvent was removed under reduced pressure. After purification by flash chromatography (EtOAc–petroleum ether = 1/4) and recrystallization of EtOAc–petroleum ether, the methylated product 4-methoxy-6-methyl-2H-pyran-2-one (9.3 g, 84%) was obtained as a white solid. ¹H NMR (400 MHz, CDCl₃): δ_H 5.74 (1H, d, *J* = 2.0 Hz), 5.37 (1H, d, *J* = 2.0 Hz), 3.75 (3H, s), 2.17 (3H, s).

Synthesis of 4-methoxy-2-oxo-2H-pyran-6-carbaldehyde (3)²³

Under nitrogen, 4-methoxy-6-methyl-2H-pyran-2-one (2) (5.6 g, 40 mmol) and SeO₂ (22 g, 200.0 mmol) were dissolved in dry dioxane (150 mL), inside a sealed tube. The mixture was heated to 160 °C for 4 h. Then, the reaction was cooled to room temperature and filtered, and the filter cake was washed with EtOAc (30 mL). The crude product was purified by flash chromatography (EtOAc–petroleum ether = 1/1) to afford the aldehyde (3) (5.6 g, 91%) as a yellowish solid. ¹H NMR (400 MHz, CDCl₃): δ_H 9.51 (1H, s), 6.67 (1H, s), 5.74 (1H, s), 3.86 (3H, s).

Synthesis of (E)-3-(4-methoxy-2-oxo-2H-pyran-6-yl)acrylic acid (4)³⁶

A solution of aldehyde (3) (3.08 g, 20.0 mmol), malonic acid (2.08 g, 20.0 mmol) in pyridine (10 mL, 120 mmol) and piperidine (0.1 mL) was heated to reflux for 3 h. The resulting solution was poured into 2 M aq. HCl and cooled to room temperature. The solid was filtered and washed with water.

The crude product was purified by flash chromatography (MeOH–dichloromethane = 3/50) to afford the acrylic acid (4) (1.84 g, 47%) as a yellow solid. ¹H NMR (400 MHz, DMSO): δ_H 7.23 (1H, dd, *J* = 15.7, 2.6 Hz), 6.71 (1H, s), 6.41 (1H, dd, *J* = 15.7, 2.8 Hz), 5.79 (1H, s), 3.84 (3H, s); ¹³C NMR (100 MHz, DMSO): δ_C 169.9, 166.3, 162.0, 155.3, 133.9, 124.1, 106.3, 91.2, 56.6; MS (ESI): *m/z* 195.0 [M – H][–]; HRMS (ESI): *m/z* calcd for C₉H₈O₅ [M – H][–], 195.0299; found, 195.0293.

General procedure for the preparation of (E)-phenethyl-3-(4-methoxy-2-oxo-2H-pyran-6-yl)acrylate and its derivatives (5a–u)³⁷

To a stirred solution of acrylic acid (4) (0.3 mmol) in CH₂Cl₂ (3 mL) were added EDC·HCl (1.2 eq.), DMAP (0.1 eq.), and the corresponding phenethyl alcohol (1.2 eq.), and the resulting mixture was stirred at room temperature overnight. The solvent was removed under reduced pressure, and the residue was purified by flash chromatography (EtOAc–petroleum ether = 1/3) to give the corresponding ester (5a–u).

Synthesis of (E)-phenethyl-3-(4-methoxy-2-oxo-2H-pyran-6-yl)acrylate (5a)

Following the general procedure, 5a was obtained as a white solid (54.1 mg, 60%). ¹H NMR (400 MHz, CDCl₃): δ_H 7.22–7.33 (5H, m), 7.06 (1H, d, *J* = 15.6 Hz), 6.70 (1H, d, *J* = 15.5 Hz), 6.10 (1H, d, *J* = 2.0 Hz), 5.58 (1H, d, *J* = 2.1 Hz), 4.41 (2H, t, *J* = 6.9 Hz), 3.83 (3H, s), 2.99 (2H, t, *J* = 6.9 Hz); ¹³C NMR (100 MHz, CDCl₃): δ_C 169.9, 165.6, 162.8, 155.6, 137.6, 133.8, 128.9, 128.5, 126.6, 124.5, 106.1, 91.3, 65.6, 56.2, 35.0; MS (ESI): *m/z* 301.1 [M + H]⁺; HRMS (ESI): *m/z* calcd for C₁₇H₁₆O₅Na [M + Na]⁺, 323.0890; found, 323.0921.

Synthesis of (E)-2-chlorophenethyl-3-(4-methoxy-2-oxo-2H-pyran-6-yl)acrylate (5b)

Following the general procedure, 5b was obtained as a white solid (68.1 mg, 68%). ¹H NMR (400 MHz, CDCl₃): δ_H 7.37 (1H, dd, *J* = 7.2, 1.9 Hz), 7.28–7.18 (3H, m), 7.07 (1H, d, *J* = 15.6 Hz),

6.69 (1H, d, $J = 15.5$ Hz), 6.10 (1H, d, $J = 2.1$ Hz), 5.58 (1H, d, $J = 2.2$ Hz), 4.44 (2H, t, $J = 6.8$ Hz), 3.84 (3H, s), 3.14 (2H, t, $J = 6.8$ Hz); ^{13}C NMR (100 MHz, CDCl_3): δ_{C} 169.9, 165.6, 162.8, 155.6, 135.3, 134.2, 133.9, 131.2, 129.6, 128.2, 126.9, 124.4, 106.2, 91.4, 63.9, 56.2, 32.8; MS (ESI): m/z 335.1 $[\text{M} + \text{H}]^+$; HRMS (ESI): m/z calcd for $\text{C}_{17}\text{H}_{15}\text{ClO}_5\text{Na}$ $[\text{M} + \text{Na}]^+$, 357.0500; found, 357.0522.

Synthesis of (*E*)-3-chlorophenethyl-3-(4-methoxy-2-oxo-2H-pyran-6-yl)acrylate (5c)

Following the general procedure, **5c** was obtained as a white solid (52.1 mg, 52%). ^1H NMR (400 MHz, CDCl_3): δ_{H} 7.28–7.20 (3H, m), 7.12 (1H, dt, $J = 6.7, 1.7$ Hz), 7.06 (1H, d, $J = 15.6$ Hz), 6.69 (1H, d, $J = 15.5$ Hz), 6.12 (1H, d, $J = 2.1$ Hz), 5.59 (1H, d, $J = 2.2$ Hz), 4.40 (2H, t, $J = 6.8$ Hz), 3.84 (3H, s), 2.97 (2H, t, $J = 6.8$ Hz); ^{13}C NMR (100 MHz, CDCl_3): δ_{C} 169.9, 165.5, 162.8, 155.6, 139.7, 134.0, 134.0, 129.8, 129.0, 127.1, 126.9, 124.3, 106.3, 91.4, 65.1, 56.2, 34.7; MS (ESI): m/z 335.1 $[\text{M} + \text{H}]^+$; HRMS (ESI): m/z calcd for $\text{C}_{17}\text{H}_{15}\text{ClO}_5\text{Na}$ $[\text{M} + \text{Na}]^+$, 357.0500; found, 357.0529.

Synthesis of (*E*)-4-chlorophenethyl-3-(4-methoxy-2-oxo-2H-pyran-6-yl)acrylate (5d)

Following the general procedure, **5d** was obtained as a white solid (65.1 mg, 65%). ^1H NMR (400 MHz, CDCl_3): δ_{H} 7.28 (2H, d, $J = 8.4$ Hz), 7.17 (2H, d, $J = 8.3$ Hz), 7.06 (1H, d, $J = 15.5$ Hz), 6.69 (1H, d, $J = 15.5$ Hz), 6.11 (1H, d, $J = 2.0$ Hz), 5.59 (1H, d, $J = 2.1$ Hz), 4.38 (2H, t, $J = 6.8$ Hz), 3.84 (3H, s), 2.96 (2H, t, $J = 6.8$ Hz); ^{13}C NMR (100 MHz, CDCl_3): δ_{C} 169.9, 165.5, 162.8, 155.6, 136.1, 134.0, 132.5, 130.2, 128.7, 124.3, 106.2, 91.4, 65.2, 56.2, 34.4; MS (ESI): m/z 335.0 $[\text{M} + \text{H}]^+$; HRMS (ESI): m/z calcd for $\text{C}_{17}\text{H}_{15}\text{ClO}_5\text{Na}$ $[\text{M} + \text{Na}]^+$, 357.0500; found, 357.0519.

Synthesis of (*E*)-2-methylphenethyl-3-(4-methoxy-2-oxo-2H-pyran-6-yl)acrylate (5e)

Following the general procedure, **5e** was obtained as a white solid (51.8 mg, 55%). ^1H NMR (400 MHz, CDCl_3): δ_{H} 7.20–7.12 (4H, m), 7.07 (1H, d, $J = 15.6$ Hz), 6.70 (1H, d, $J = 15.5$ Hz), 6.10 (1H, d, $J = 2.1$ Hz), 5.58 (1H, d, $J = 2.2$ Hz), 4.38 (2H, t, $J = 7.2$ Hz), 3.83 (3H, s), 3.00 (2H, t, $J = 7.2$ Hz), 2.36 (3H, s); ^{13}C NMR (100 MHz, CDCl_3): δ_{C} 169.9, 165.6, 162.8, 155.7, 136.4, 135.6, 133.8, 130.4, 129.6, 126.8, 126.1, 124.5, 106.1, 91.4, 64.7, 56.1, 32.3, 19.3; MS (ESI): m/z 315.1 $[\text{M} + \text{H}]^+$; HRMS (ESI): m/z calcd for $\text{C}_{18}\text{H}_{18}\text{O}_5\text{Na}$ $[\text{M} + \text{Na}]^+$, 337.1046; found, 337.1062.

Synthesis of (*E*)-3-methylphenethyl-3-(4-methoxy-2-oxo-2H-pyran-6-yl)acrylate (5f)

Following the general procedure, **5f** was obtained as a white solid (52.8 mg, 56%). ^1H NMR (400 MHz, CDCl_3): δ_{H} 7.20 (1H, t, $J = 7.8$ Hz), 7.02–7.08 (4H, m), 6.71 (1H, d, $J = 15.5$ Hz), 6.10 (1H, d, $J = 2.1$ Hz), 5.58 (1H, d, $J = 2.2$ Hz), 4.40 (2H, t, $J = 7.0$ Hz), 3.83 (3H, s), 2.95 (2H, t, $J = 7.0$ Hz), 2.34 (3H, s); ^{13}C NMR (100 MHz, CDCl_3): δ_{C} 169.9, 165.6, 162.8, 155.7, 138.1, 137.5, 133.8, 129.7, 128.4, 127.4, 125.9, 124.6, 106.1, 91.3, 65.7, 56.1, 35.0, 21.3; MS (ESI): m/z 315.2 $[\text{M} + \text{H}]^+$; HRMS (ESI): m/z calcd for $\text{C}_{18}\text{H}_{18}\text{O}_5\text{Na}$ $[\text{M} + \text{Na}]^+$, 337.1046; found, 337.1069.

Synthesis of (*E*)-4-methoxyphenethyl-3-(4-methoxy-2-oxo-2H-pyran-6-yl)acrylate (5g)

Following the general procedure, **5g** was obtained as a white solid (63.9 mg, 71%). ^1H NMR (400 MHz, CDCl_3): δ_{H} 7.15 (2H, d, $J = 8.6$ Hz), 7.06 (1H, d, $J = 15.6$ Hz), 6.86 (2H, d, $J = 8.6$ Hz), 6.71 (1H, d, $J = 15.5$ Hz), 6.10 (1H, d, $J = 2.1$ Hz), 5.58 (1H, d, $J = 2.1$ Hz), 4.37 (2H, t, $J = 6.9$ Hz), 3.84 (3H, s), 3.80 (3H, s), 2.93 (2H, t, $J = 6.9$ Hz); ^{13}C NMR (100 MHz, CDCl_3): δ_{C} 170.0, 165.6, 162.8, 158.4, 155.7, 133.8, 129.9, 129.6, 124.6, 114.0, 106.1, 91.3, 65.8, 56.2, 55.2, 34.2; MS (ESI): m/z 353.2 $[\text{M} + \text{Na}]^+$; HRMS (ESI): m/z calcd for $\text{C}_{18}\text{H}_{18}\text{O}_6\text{Na}$ $[\text{M} + \text{Na}]^+$, 353.0996; found, 353.1026.

Synthesis of (*E*)-2-(piperidin-1-yl)ethyl-3-(4-methoxy-2-oxo-2H-pyran-6-yl)acrylate (5h)

Following the general procedure, **5h** was obtained as a white solid (50.0 mg, 51%). ^1H NMR (400 MHz, CDCl_3): δ_{H} 7.10 (1H, d, $J = 15.6$ Hz), 6.74 (1H, d, $J = 15.6$ Hz), 6.12 (1H, d, $J = 2.1$ Hz), 5.58 (1H, d, $J = 2.2$ Hz), 4.33 (2H, t, $J = 6.0$ Hz), 3.84 (3H, s), 2.67 (2H, t, $J = 6.0$ Hz), 2.47 (4H, t, $J = 4.9$ Hz), 1.59 (4H, dt, $J = 11.1, 5.6$ Hz), 1.44 (2H, dt, $J = 10.3, 4.7$ Hz); ^{13}C NMR (100 MHz, CDCl_3): δ_{C} 169.9, 165.6, 162.8, 155.7, 133.8, 124.6, 106.1, 91.3, 62.9, 57.2, 56.1, 54.8, 25.9, 24.1; MS (ESI): m/z 308.1 $[\text{M} + \text{H}]^+$.

Synthesis of (*E*)-2-(pyridin-2-yl)ethyl-3-(4-methoxy-2-oxo-2H-pyran-6-yl)acrylate (5i)

Following the general procedure, **5i** was obtained as a white solid (45.0 mg, 50%). ^1H NMR (400 MHz, CDCl_3): δ_{H} 8.56 (1H, d, $J = 4.8$ Hz), 7.64 (1H, td, $J = 7.7, 1.8$ Hz), 7.24–7.12 (2H, m), 7.06 (1H, d, $J = 15.6$ Hz), 6.67 (1H, d, $J = 15.5$ Hz), 6.10 (1H, d, $J = 2.1$ Hz), 5.58 (1H, d, $J = 2.1$ Hz), 4.60 (2H, t, $J = 6.6$ Hz), 3.83 (3H, s), 3.17 (2H, t, $J = 6.6$ Hz); ^{13}C NMR (100 MHz, CDCl_3): δ_{C} 170.0, 165.6, 162.8, 157.8, 155.6, 149.5, 136.5, 133.8, 124.4, 123.5, 121.7, 106.1, 91.3, 64.2, 56.2, 37.3. MS (ESI): m/z 302.1 $[\text{M} + \text{H}]^+$; HRMS (ESI): m/z calcd for $\text{C}_{16}\text{H}_{21}\text{NO}_5\text{Na}$ $[\text{M} + \text{Na}]^+$, 324.0842; found, 324.0860.

Synthesis of (*E*)-2-morpholinoethyl-3-(4-methoxy-2-oxo-2H-pyran-6-yl)acrylate (5j)

Following the general procedure, **5j** was obtained as a white solid (52.9 mg, 57%). ^1H NMR (400 MHz, CDCl_3): δ_{H} 7.10 (1H, d, $J = 15.5$ Hz), 6.74 (1H, d, $J = 15.5$ Hz), 6.13 (1H, d, $J = 2.1$ Hz), 5.59 (1H, d, $J = 2.2$ Hz), 4.34 (2H, t, $J = 5.7$ Hz), 3.84 (3H, s), 3.72 (4H, t, $J = 4.6$ Hz), 2.70 (2H, t, $J = 5.7$ Hz), 2.54 (4H, t, $J = 4.6$ Hz); ^{13}C NMR (100 MHz, CDCl_3): δ_{C} 169.9, 165.6, 162.7, 155.6, 134.0, 124.4, 106.2, 91.4, 66.8, 62.3, 57.0, 56.2, 53.8; MS (ESI): m/z 310.2 $[\text{M} + \text{H}]^+$; HRMS (ESI): m/z calcd for $\text{C}_{15}\text{H}_{19}\text{NO}_6$ $[\text{M} + \text{H}]^+$, 310.1285; found, 310.1281.

Synthesis of (*E*)-2-(thiophen-2-yl)ethyl-3-(4-methoxy-2-oxo-2H-pyran-6-yl)acrylate (5k)

Following the general procedure, **5k** was obtained as a white solid (63.4 mg, 69%). ^1H NMR (400 MHz, CDCl_3): δ_{H} 7.17 (1H, dd, $J = 5.1, 1.1$ Hz), 7.10 (1H, d, $J = 15.6$ Hz), 6.95 (1H, dd, $J =$

5.1, 3.5 Hz), 6.88 (1H, dd, $J = 3.4, 0.9$ Hz), 6.73 (1H, d, $J = 15.5$ Hz), 6.12 (1H, d, $J = 2.1$ Hz), 5.59 (1H, d, $J = 2.1$ Hz), 4.42 (2H, t, $J = 6.7$ Hz), 3.84 (3H, s), 3.21 (2H, t, $J = 6.6$ Hz); ^{13}C NMR (100 MHz, CDCl_3): δ_{C} 169.9, 165.5, 162.7, 155.6, 139.6, 134.0, 126.9, 125.6, 124.4, 124.1, 106.2, 91.4, 65.2, 56.1, 29.2; MS (ESI): m/z 307.0 $[\text{M} + \text{H}]^+$; HRMS (ESI): m/z calcd for $\text{C}_{15}\text{H}_{14}\text{O}_5\text{SNa}$ $[\text{M} + \text{Na}]^+$, 329.0454; found, 329.0465.

Synthesis of (*E*)-2-(4-methylthiazol-5-yl)ethyl-3-(4-methoxy-2-oxo-2H-pyran-6-yl)acrylate (5l)

Following the general procedure, **5l** was obtained as a white solid (60.7 mg, 63%). ^1H NMR (400 MHz, CDCl_3): δ_{H} 8.60 (1H, s), 7.10 (1H, d, $J = 15.5$ Hz), 6.71 (1H, d, $J = 15.5$ Hz), 6.13 (1H, d, $J = 2.1$ Hz), 5.60 (1H, d, $J = 2.1$ Hz), 4.37 (2H, t, $J = 6.6$ Hz), 3.84 (3H, s), 3.16 (2H, t, $J = 6.6$ Hz), 2.43 (3H, s); ^{13}C NMR (100 MHz, CDCl_3): δ_{C} 169.9, 165.4, 162.7, 155.5, 150.0, 149.9, 134.3, 126.4, 124.0, 106.4, 91.5, 64.6, 56.2, 25.8, 14.9; MS (ESI): m/z 344.1 $[\text{M} + \text{Na}]^+$; HRMS (ESI): m/z calcd for $\text{C}_{15}\text{H}_{15}\text{NO}_5\text{SNa}$ $[\text{M} + \text{Na}]^+$, 344.0563; found, 344.0581.

Synthesis of (*E*)-2-fluorophenethyl-3-(4-methoxy-2-oxo-2H-pyran-6-yl)acrylate (5m)

Following the general procedure, **5m** was obtained as a white solid (60.1 mg, 63%). ^1H NMR (400 MHz, CDCl_3): δ_{H} 7.26–7.18 (2H, m), 7.12–6.99 (3H, m), 6.68 (1H, d, $J = 15.5$ Hz), 6.11 (1H, d, $J = 2.1$ Hz), 5.59 (1H, d, $J = 2.1$ Hz), 4.41 (2H, t, $J = 6.8$ Hz), 3.83 (3H, s), 3.04 (2H, t, $J = 6.7$ Hz); ^{13}C NMR (100 MHz, CDCl_3): δ_{C} 169.9, 165.5, 162.7 (d, $J = 33.6$ Hz), 160.0, 155.6, 133.9, 131.2 (d, $J = 4.5$ Hz), 128.5 (d, $J = 8.2$ Hz), 124.5 (d, $J = 15.8$ Hz), 124.4, 124.1 (d, $J = 3.5$ Hz), 115.3 (d, $J = 21.8$ Hz), 106.2, 91.3, 64.3, 56.2, 28.5; MS (ESI): m/z 319.1 $[\text{M} + \text{H}]^+$; HRMS (ESI): m/z calcd for $\text{C}_{17}\text{H}_{15}\text{FO}_5\text{Na}$ $[\text{M} + \text{Na}]^+$, 341.0796; found, 341.0825.

Synthesis of (*E*)-2-bromophenethyl-3-(4-methoxy-2-oxo-2H-pyran-6-yl)acrylate (5n)

Following the general procedure, **5n** was obtained as a white solid (77.1 mg, 68%). ^1H NMR (400 MHz, CDCl_3): δ_{H} 7.55 (1H, d, $J = 7.9$ Hz), 7.27 (2H, d, $J = 4.3$ Hz), 7.14–7.05 (2H, m), 6.69 (1H, d, $J = 15.6$ Hz), 6.11 (1H, d, $J = 2.1$ Hz), 5.59 (1H, d, $J = 2.1$ Hz), 4.44 (2H, t, $J = 6.8$ Hz), 3.83 (3H, s), 3.15 (2H, t, $J = 6.8$ Hz); ^{13}C NMR (100 MHz, CDCl_3): δ_{C} 169.9, 165.5, 162.8, 155.6, 137.0, 133.9, 132.9, 131.2, 128.5, 127.6, 124.6, 124.3, 106.2, 91.4, 64.0, 56.2, 35.2; MS (ESI): m/z 379.1 $[\text{M} + \text{H}]^+$; HRMS (ESI): m/z calcd for $\text{C}_{17}\text{H}_{15}\text{BrO}_5\text{Na}$ $[\text{M} + \text{Na}]^+$, 400.9995; found, 401.0025.

Synthesis of (*E*)-2,6-dichlorophenethyl-3-(4-methoxy-2-oxo-2H-pyran-6-yl)acrylate (5o)

Following the general procedure, **5o** was obtained as a white solid (69.6 mg, 63%). ^1H NMR (400 MHz, CDCl_3): δ_{H} 7.31 (2H, d, $J = 8.0$ Hz), 7.14 (1H, d, $J = 7.9$ Hz), 7.09 (1H, d, $J = 15.7$ Hz), 6.67 (1H, d, $J = 15.5$ Hz), 6.11 (1H, d, $J = 2.0$ Hz), 5.59 (1H, d, $J = 2.1$ Hz), 4.45 (2H, t, $J = 6.8$ Hz), 3.84 (3H, s), 3.37 (2H, t, $J = 6.8$ Hz); ^{13}C NMR (100 MHz, CDCl_3): δ_{C} 169.9, 165.5, 162.8, 155.7, 135.9, 133.9, 133.6, 128.5, 128.3, 124.4, 106.2, 91.3, 62.6,

56.2, 30.4; MS (ESI): m/z 391.0 $[\text{M} + \text{Na}]^+$; HRMS (ESI): m/z calcd for $\text{C}_{17}\text{H}_{14}\text{Cl}_2\text{O}_5\text{Na}$ $[\text{M} + \text{Na}]^+$, 391.0111; found, 391.0131.

Synthesis of (*E*)-2-methoxyphenethyl-3-(4-methoxy-2-oxo-2H-pyran-6-yl)acrylate (5p)

Following the general procedure, **5p** was obtained as a white solid (68.3 mg, 69%). ^1H NMR (400 MHz, CDCl_3): δ_{H} 7.25–7.14 (2H, m), 7.05 (1H, d, $J = 15.6$ Hz), 6.92–6.83 (2H, m), 6.69 (1H, d, $J = 15.6$ Hz), 6.09 (1H, d, $J = 2.1$ Hz), 5.58 (1H, d, $J = 2.1$ Hz), 4.39 (2H, t, $J = 6.9$ Hz), 3.82 (6H, s), 3.01 (2H, t, $J = 6.9$ Hz); ^{13}C NMR (100 MHz, CDCl_3): δ_{C} 170.0, 165.7, 162.9, 157.6, 155.7, 133.6, 130.8, 128.0, 125.8, 124.7, 120.4, 110.3, 106.0, 91.3, 64.5, 56.1, 55.2, 29.9; MS (ESI): m/z 331.2 $[\text{M} + \text{H}]^+$; HRMS (ESI): m/z calcd for $\text{C}_{18}\text{H}_{18}\text{O}_6\text{Na}$ $[\text{M} + \text{Na}]^+$, 353.0996; found, 353.1017.

Synthesis of (*E*)-2-(trifluoromethyl)phenethyl-3-(4-methoxy-2-oxo-2H-pyran-6-yl)acrylate (5q)

Following the general procedure, **5q** was obtained as a white solid (56.3 mg, 51%). ^1H NMR (400 MHz, CDCl_3): δ_{H} 7.66 (1H, d, $J = 7.8$ Hz), 7.51 (1H, t, $J = 7.4$ Hz), 7.43–7.32 (2H, m), 7.08 (1H, d, $J = 15.6$ Hz), 6.70 (1H, d, $J = 15.6$ Hz), 6.12 (1H, d, $J = 2.0$ Hz), 5.59 (1H, d, $J = 2.1$ Hz), 4.43 (2H, t, $J = 6.8$ Hz), 3.84 (3H, s), 3.19 (2H, t, $J = 6.7$ Hz); ^{13}C NMR (100 MHz, CDCl_3): δ_{C} 169.9, 165.5, 162.8, 155.6, 136.1, 134.0, 131.8, 131.8, 128.8, 126.9, 126.2 (q, $J = 5.6$ Hz, 11.1 Hz), 124.3, 106.2, 91.4, 64.9, 56.2, 31.8; MS (ESI): m/z 369.2 $[\text{M} + \text{H}]^+$; HRMS (ESI): m/z calcd for $\text{C}_{18}\text{H}_{15}\text{F}_3\text{O}_5\text{Na}$ $[\text{M} + \text{Na}]^+$, 391.0764; found, 391.0798.

Synthesis of (*E*)-2-nitrophenethyl-3-(4-methoxy-2-oxo-2H-pyran-6-yl)acrylate (5r)

Following the general procedure, **5r** was obtained as a white solid (72.5 mg, 70%). ^1H NMR (400 MHz, CDCl_3): δ_{H} 7.97 (1H, d, $J = 8.16$ Hz), 7.58 (1H, td, $J = 7.5, 1.1$ Hz), 7.46–7.39 (2H, m), 7.06 (1H, d, $J = 15.6$ Hz), 6.66 (1H, d, $J = 15.6$ Hz), 6.14 (1H, d, $J = 2.0$ Hz), 5.59 (1H, d, $J = 2.1$ Hz), 4.51 (2H, t, $J = 6.4$ Hz), 3.84 (3H, s), 3.32 (2H, t, $J = 6.3$ Hz); ^{13}C NMR (100 MHz, CDCl_3): δ_{C} 170.0, 165.4, 162.8, 155.5, 149.6, 134.1, 133.1, 132.8, 132.8, 128.0, 125.0, 124.0, 106.3, 91.4, 64.5, 56.2, 32.3; MS (ESI): m/z 346.2 $[\text{M} + \text{H}]^+$; HRMS (ESI): m/z calcd for $\text{C}_{17}\text{H}_{15}\text{NO}_7\text{Na}$ $[\text{M} + \text{Na}]^+$, 368.0741; found, 368.0772.

Synthesis of (*E*)-2,4-dichlorophenethyl-3-(4-methoxy-2-oxo-2H-pyran-6-yl)acrylate (5s)

Following the general procedure, **5s** was obtained as a white solid (71.8 mg, 65%). ^1H NMR (400 MHz, CDCl_3): δ_{H} 7.39 (1H, s), 7.20 (2H, d, $J = 1.4$ Hz), 7.07 (1H, d, $J = 15.5$ Hz), 6.67 (1H, d, $J = 15.5$ Hz), 6.12 (1H, d, $J = 2.1$ Hz), 5.59 (1H, d, $J = 2.2$ Hz), 4.41 (2H, t, $J = 6.7$ Hz), 3.84 (3H, s), 3.10 (2H, t, $J = 6.7$ Hz); ^{13}C NMR (100 MHz, CDCl_3): δ_{C} 169.9, 165.5, 162.8, 155.5, 134.8, 134.0, 133.9, 133.3, 131.9, 129.4, 127.2, 124.1, 106.3, 91.4, 63.6, 56.2, 32.2; MS (ESI): m/z 369.0 $[\text{M} + \text{H}]^+$; HRMS (ESI): m/z calcd for $\text{C}_{17}\text{H}_{14}\text{Cl}_2\text{O}_5\text{Na}$ $[\text{M} + \text{Na}]^+$, 391.0111; found, 391.0143.

Synthesis of (*E*)-2,4,6-trimethylphenethyl-3-(4-methoxy-2-oxo-2H-pyran-6-yl)acrylate (**5t**)

Following the general procedure, **5t** was obtained as a white solid (50.3 mg, 49%). ¹H NMR (400 MHz, CDCl₃): δ_H 7.09 (1H, d, *J* = 15.5 Hz), 6.85 (2H, s), 6.70 (1H, d, *J* = 15.5 Hz), 6.11 (1H, d, *J* = 2.0 Hz), 5.59 (1H, d, *J* = 2.1 Hz), 4.27 (2H, t, *J* = 7.7 Hz), 3.84 (3H, s), 3.02 (2H, t, *J* = 7.7 Hz), 2.34 (6H, s), 2.25 (3H, s); ¹³C NMR (100 MHz, CDCl₃): δ_C 169.9, 165.7, 162.8, 155.7, 136.8, 136.0, 133.9, 130.6, 129.1, 124.5, 106.2, 91.4, 63.8, 56.2, 28.5, 20.8, 19.9; MS (ESI): *m/z* 365.2 [M + Na]⁺; HRMS (ESI): *m/z* calcd for C₂₀H₂₂O₅Na [M + Na]⁺, 365.1359; found, 365.1390.

Synthesis of (*E*)-2-(naphthalen-1-yl)ethyl-3-(4-methoxy-2-oxo-2H-pyran-6-yl)acrylate (**5u**)

Following the general procedure, **5u** was obtained as a white solid (60.9 mg, 58%). ¹H NMR (400 MHz, CDCl₃): δ_H 8.10 (1H, d, *J* = 8.3 Hz), 7.86 (1H, d, *J* = 7.8 Hz), 7.76 (1H, d, *J* = 7.8 Hz), 7.58–7.36 (4H, m), 7.02 (1H, d, *J* = 15.6 Hz), 6.69 (1H, d, *J* = 15.6 Hz), 6.06 (1H, d, *J* = 2.0 Hz), 5.57 (1H, d, *J* = 2.1 Hz), 4.53 (2H, t, *J* = 7.2 Hz), 3.82 (3H, s), 3.46 (2H, t, *J* = 7.2 Hz); ¹³C NMR (100 MHz, CDCl₃): δ_C 169.9, 165.6, 162.6, 155.6, 133.9, 133.5, 132.0, 130.9, 128.9, 127.5, 127.1, 126.2, 125.7, 125.5, 124.4, 123.5, 106.2, 91.4, 65.1, 56.1, 32.1; MS (ESI): *m/z* 351.2 [M + H]⁺; HRMS (ESI): *m/z* calcd for C₂₁H₁₈NO₅Na [M + Na]⁺, 373.1046; found, 373.1072.

Cell culture

HeLa, HSC-2, and A549 cell lines were kindly provided by Professor Li Haiou (Japan). MCF-7 and C6 were purchased from the Center of Experiment Animal of Sun Yat-sen University (Guangzhou, China). Cells were cultured in Dulbecco's modified Eagle's medium (Gibco) supplemented with 10% (v/v) fetal bovine serum (Hyclone), 100 U mL⁻¹ of penicillin, and 100 μg mL⁻¹ of streptomycin (Hyclone). These cells were grown in a humidified incubator containing 5% CO₂ at 37 °C and subcultured every three days.

Antiproliferative assays

These derivatives were evaluated for their antiproliferative activities in five different cancer cell lines by MTT assay. Cells in log-phase were plated into 96-well plates with a density of 3.5 × 10⁴ cells mL⁻¹ overnight at 37 °C. Cells were then treated with various concentrations of compounds and incubated at 37 °C for an additional 48 h. The antiproliferative activities of compounds were evaluated by MTT assay. In brief, 20 μL of MTT reagent was added to each well and the plates continued to incubate for another 4 h at 37 °C. Formazan crystals were dissolved in 120 μL of DMSO. The optical density was assayed at 490 nm with an automated micro-plate reader (Thermo, Multiskan Ascent, USA) and the 50% inhibition concentration was determined from a dose–response curve.

Cell cycle analysis

HeLa cells (2 × 10⁵ cells per well) were seeded into 6-well plates for 24 h. Compound **5o** was added into each well in

various concentrations (0.5, 1, 2 μM). Cells were harvested with trypsin and fixed with ice-cold 70% EtOH at 4 °C overnight. EtOH was washed with ice-cold PBS buffer. Finally, samples were stained with a Cell Cycle and Apoptosis Analysis Kit (Beyotime, China) for 30 min at 37 °C. The DNA contents of 11 000 events were measured by flow cytometry (Beckman Coulter, Epics XL, USA).

Cell apoptosis assay

Cell apoptosis assay was assessed by using an Annexin V-FITC/PI staining assay kit (Becton Dickinson, USA). The cells were treated with **5o** at concentrations of 0.5, 1 and 2 μM for 24 h. Both detached and attached cells were harvested with trypsin, washed with cold phosphate-buffered saline (PBS), and then resuspended in 100 μL binding buffer. Five μL each of Annexin V-FITC solution and PI were added. The cells were incubated at room temperature for 15 min and analyzed by flow cytometry within 1 h.

Immunofluorescence assay

HeLa cells (4 × 10⁴ cells per well) were seeded on glass-bottom cell culture dishes for 24 h. After incubation in the presence or absence of **5o** (0.5, 1 μM), cells were fixed in 4% paraformaldehyde, permeabilized with 0.5% Triton X-100 and 0.05% Tween-20, blocked for 1 h and immunostained with rabbit anti-β-actin (1 : 400; Cell Signaling Technology) overnight at 4 °C. Subsequently, the antibodies were removed and the cells were washed with PBS. The cells were incubated with CF488-conjugated goat-anti-rabbit IgG (1 : 700), highly cross-absorbed (Biotium, USA). Nuclei were stained with Hoechst 33342 (5 mg mL⁻¹). Fluorescence images were captured under a Zeiss fluorescence microscope (Zeiss, LSM710, Germany).

Migration and invasion assay

In vitro migration and invasion assays were carried out using 24-well plates with 8 μm pore size inserts (Transwell, Corning, USA). Only for the invasion assay, the upper chamber was coated with 100 μL diluted Matrigel (0.5 mg mL⁻¹). A serum-free DMEM cell suspension (100 μL, 3 × 10⁵ cells mL⁻¹) with/without **5o** (0.5, 1 μM) was added in the upper chamber. A medium (600 μL) with 10% FBS was added to the lower chamber. After 36 h of incubation, cells were fixed with 4% formaldehyde and stained with 0.1% crystal violet. Then, cells on the upper membrane surface were removed with cotton swabs. Stained cells were photographed under a microscope.

Western blot assay

Treated cells were lysed with RIPA lysis buffer (P0013, Beyotime, China). The total protein quality was determined by using a BCA Protein Assay Kit (Pierce; Rockford IL, USA). Proteins were denatured and separated by 10% SDS-PAGE and then electrotransferred to polyvinylidene difluoride membranes (Immobilon PVDF, Millipore, Bedford). The membranes were washed with Tris-Buffered Saline and Tween 20 (TBST) and then blocked for 2 h at room temperature. The membranes were then incubated with special antibodies

against β -tubulin, caspase 3, PARP, CyclinB1, Cdc25c, and Cdc2 (Cell Signaling Technology, USA) at 4 °C overnight and washed with TBST. Later, the membranes were incubated with anti-rabbit horseradish peroxidase-conjugated secondary antibodies (1:5000) for 1 h at room temperature and then washed with TBST. Protein bands were detected by using an enhanced chemiluminescence detection system (Westar Super-nova, Cyanogen, Italy) and recorded on an X-ray film (Fujifilm; Tokyo, Japan).

ADMET prediction

ADMET refers to absorption, distribution, metabolism, excretion, and toxicity properties of the drug in the body. We use the ADMET descriptor module in Discovery studio (version 2.5, Accelrys Inc., San Diego, CA) to predict the ADMET properties according to the molecular structure. The ADMET descriptor module estimates the aqueous solubility, blood-brain barrier (BBB) penetration, cytochrome P450 (CYP450) 2D6 inhibition, hepatotoxicity, human intestinal absorption (HIA) and plasma protein binding of a set of compounds.

Acknowledgements

This work was funded in part by the National Natural Science Foundation of China (no. 81173470, 81473138, 81172941), the National High-tech R&D Program of China (863 Program) (2012AA020307), and the introduction of Innovative R&D Team Program of Guangdong Province (no. 2009010058). Partial support is also due to NIH grant CA177584 from the National Cancer Institute awarded to K.H. Lee.

References

- 1 R. Siegel, J. Ma, Z. Zhou and A. Jemal, *CA-Cancer J. Clin.*, 2014, **64**, 9–29.
- 2 R. Siegel, D. Naishadham and A. Jemal, *CA-Cancer J. Clin.*, 2013, **63**, 11–30.
- 3 M. F. Tolba, S. S. Azab, A. E. Khalifa, S. Z. Abdel-Rahman and A. B. Abdel-Naim, *IUBMB Life*, 2013, **65**, 699–709.
- 4 (a) G. Ozturk, Z. Ginis, S. Akyol, G. Erden, A. Gurel and O. Akyol, *Eur. Rev. Med. Pharmacol. Sci.*, 2012, **16**, 2064–2068; (b) M. Watabe, K. Hishikawa, A. Takayanagi and N. Shimizu, *J. Biol. Chem.*, 2004, **279**, 6017–6026.
- 5 T. Nagaoka, A. H. Banskota, Y. Tezuka, I. Saiki and S. Kadota, *Bioorg. Med. Chem.*, 2002, **10**, 3351–3359.
- 6 W. L. Lin, W. H. Liang, Y. J. Lee, S. K. Chuang and T. H. Tseng, *Chem. Biol. Interact.*, 2010, **188**, 607–615.
- 7 (a) J. H. Chen, Y. Shao, M. T. Huang, C. K. Chin and C. T. Ho, *Cancer Lett.*, 1996, **108**, 211–214; (b) Y. J. Chen, M. S. Shiao, M. L. Hsu, T. H. Tsai and S. Y. Wang, *J. Agric. Food Chem.*, 2001, **49**, 5615–5619.
- 8 Y. J. Lee, P. H. Liao, W. K. Chen and C. C. Yang, *Cancer Lett.*, 2000, **153**, 51–56.
- 9 (a) J. Wu, C. Omene, J. Karkoszka, M. Bosland, J. Eckard, C. B. Klein and K. Frenkel, *Cancer Lett.*, 2011, **308**, 43–53; (b) C. O. Omene, J. Wu and K. Frenkel, *Invest. New Drugs*, 2012, **30**, 1279–1288.
- 10 A. Goel and V. J. Ram, *Tetrahedron*, 2009, **65**, 7865–7913.
- 11 S. E. Hagen, J. V. N. Vara Prasad, F. E. Boyer, J. M. Domagala, E. L. Ellsworth, C. Gjda, H. W. Hamilton, L. J. Markkoski, B. A. Steinbangh, B. D. Tait, E. A. Lunney, P. J. Tummino, D. Ferguson, D. Hupe, C. Nouhan, S. J. Gracheck, J. M. Saunders and S. V. Roest, *J. Med. Chem.*, 1997, **40**, 3707–3711.
- 12 M. D. Aytemir, U. Calis and M. Ozalp, *Arch. Pharm. Med. Chem.*, 2004, **337**, 281–288.
- 13 I. J. S. Fairlamb, L. R. Marrison, J. M. Dickinson, F. J. Lu and J. P. Schmidt, *Bioorg. Med. Chem.*, 2004, **12**, 4285–4299.
- 14 M. Kondoh, T. Usui, S. Kobayashi, K. Tsuchiya, K. Nishikawa, T. Nishikiori, T. Mayumi and H. Osada, *Cancer Lett.*, 1998, **126**, 29–32.
- 15 (a) S. J. Shaw, H. G. Menzella, D. C. Myles, M. Xian and A. B. Smith III, *Org. Biomol. Chem.*, 2007, **5**, 2753–2755; (b) H. Zhao, B. R. Kusuma and B. S. J. Blagg, *ACS Med. Chem. Lett.*, 2010, **1**, 311–315; (c) B. R. Clark, S. O. Connor, D. Fox, J. Leroy and C. Murphy, *Org. Biomol. Chem.*, 2011, **9**, 6306–6311; (d) H. Zhao, A. C. Donnelly, B. R. Kusuma, G. E. L. Brandt, D. Brown, R. A. Rajewski, G. Vielhauer, J. Holzbeierlein, M. S. Cohen and B. J. Blagg, *J. Med. Chem.*, 2011, **54**, 3839–3853; (e) N. Touisni, A. Maresca, P. C. McDonald, Y. Lou, A. Scozzafava, S. Dedhar, J. Y. Winum and C. T. Supuran, *J. Med. Chem.*, 2011, **54**, 8271–8277; (f) N. Yamamoto, A. K. Renfrew, B. J. Kim, N. S. Bryce and T. W. Hambley, *J. Med. Chem.*, 2012, **55**, 11013–11021; (g) H. Zhao, B. Yan, L. B. Peterson and B. S. Blagg, *ACS Med. Chem. Lett.*, 2012, **3**, 327–331; (h) D. Kumar, B. A. Mishra, K. P. C. Shekar, A. Kumar, K. Akamatsu, R. Kurihara and T. Ito, *Org. Biomol. Chem.*, 2013, **11**, 6675–6679; (i) I. Hyohdoh, N. Furuichi, T. Aoki, Y. Itezono, H. Shirai, S. Ozawa, F. Watanabe, M. Matsushita, M. Sakaitani, P. S. Ho, K. Takanashi, N. Harada, Y. Tomii, K. Yoshinari, K. Ori, M. Tabo, Y. Aoki, N. Shimma and H. Iikura, *ACS Med. Chem. Lett.*, 2013, **4**, 1059–1063; (j) C. Molzer, H. Huber, A. Steyrer, G. V. Ziesel, M. Wallner, H. T. Hong, J. T. Blanchfield, A. C. Bulmer and K. H. Wagner, *J. Nat. Prod.*, 2013, **76**, 1958–1965; (k) Y. Yin, X. Wu, H. W. Han, S. Sha, S. F. Wang, F. Qiao, A. M. Lu, P. C. Lv and H. L. Zhu, *Org. Biomol. Chem.*, 2014, **12**, 9157–9165; (l) J. Xiao, Q. Zhang, Y. Q. Gao, J. J. Tang, A. L. Zhang and J. M. Gao, *J. Agric. Food Chem.*, 2014, **62**, 3584–3590; (m) S. Sandhu, Y. Bansal, O. Silakari and G. Bansal, *Bioorg. Med. Chem.*, 2014, **22**, 3806–3814; (n) M. Basanagouda, V. B. Jambagi, N. N. Barigidad, S. S. Laxmeshwar, V. Devaru and Narayanachar, *Eur. J. Med. Chem.*, 2014, **74**, 225–233; (o) T. Nasr, S. Bondock and M. Youns, *Eur. J. Med. Chem.*, 2014, **76**, 539–548; (p) B. Yadagiri, U. D. Holagunda, R. Bantu, L. Nagarapu, C. G. Kumar, S. Pombala and B. Sridhar, *Eur. J. Med. Chem.*, 2014, **79**, 260–265.

- 16 M. S. Ali, Y. Tezuka, S. Awale, A. H. Banskota and S. Kadota, *J. Nat. Prod.*, 2001, **64**, 289–293.
- 17 Z. Fang, P. C. Liao, Y. L. Yang, F. L. Yang, Y. L. Chen, Y. Lam, K. F. Hua and S. H. Wu, *J. Med. Chem.*, 2010, **53**, 7967–7978.
- 18 J. Liu, D. Zhang, Y. Li, W. Chen, Z. Ruan, L. Deng, L. Wang, H. Tian, A. Yiu, C. Fan, H. Luo, S. Liu, Y. Wang, G. Xiao, L. Chen and W. Ye, *J. Med. Chem.*, 2013, **56**, 5734–5743.
- 19 X. Wang, K. F. Bastow, C.-M. Sun, Y. L. Lin, H. J. Yu, M. J. Don, T. S. Wu, S. Nakamura and K. H. Lee, *J. Med. Chem.*, 2004, **47**, 5816–5819.
- 20 R. J. Griffin, G. Fontana, B. T. Golding, S. Guiard, I. R. Hardcastle, J. J. J. Leahy, N. Martin, C. Richardson, L. Rigoreau, M. Stockley and G. C. M. Smith, *J. Med. Chem.*, 2005, **48**, 569–585.
- 21 (a) Y. H. Hsiang, R. Hertzberg, S. Hecht and L. F. Liu, *J. Biol. Chem.*, 1985, **260**, 14873–14878; (b) Y. H. Hsiang and L. F. Liu, *Cancer Res.*, 1988, **48**, 1722–1726; (c) B. L. Staker, K. Hjerrild, M. D. Feese, C. A. Behnke, A. B. Burgin Jr. and L. Stewart, *Proc. Natl. Acad. Sci. U. S. A.*, 2002, **99**, 15387–15392; (d) Y. H. Hsiang, L. F. Liu, M. E. Wall, M. C. Wani, A. W. Nicholas, G. Manikumar, S. Kirschenbaum, R. Silber and M. Potmesil, *Cancer Res.*, 1989, **49**, 4385–4389.
- 22 (a) M. J. Wang, Y. Q. Liu, L. C. Chang, C. Y. Wang, Y. L. Zhao, X. B. Zhao, K. Qian, X. Nan, L. Yang, X. M. Yang, H. Y. Hung, J. S. Yang, D. H. Kuo, M. Goto, S. L. Morris-Natschke, S. L. Pan, C. M. Teng, S. C. Kuo, T. S. Wu, Y. C. Wu and K. H. Lee, *J. Med. Chem.*, 2014, **57**, 6008–6018; (b) P. Huang, D. Wang, Y. Su, W. Huang, Y. Zhou, D. Cui, X. Zhu and D. Yan, *J. Am. Chem. Soc.*, 2014, **136**, 11748–11756; (c) H. Wang, H. Xie, J. Wu, X. Wei, L. Zhou, X. Xu and S. Zheng, *Angew. Chem., Int. Ed.*, 2014, **53**, 11532–11537; (d) J.-X. Duan, X. Cai, F. Meng, J. D. Sun, Q. Liu, D. Jung, H. Jiao, J. Matteucci, B. Jung, D. Bhupathi, D. Ahluwalia, H. Huang, C. P. Hart and M. Matteucci, *J. Med. Chem.*, 2011, **54**, 1715–1723; (e) Y. Shen, E. Jin, B. Zhang, C. J. Murphy, M. Sui, J. Zhao, J. Wang, J. Tang, M. Fan, E. V. Kirk and W. J. Murdoch, *J. Am. Chem. Soc.*, 2010, **132**, 4259–4265; (f) C. Samori, A. Guerrini, G. Varchi, G. Fontana, E. Bombardelli, S. Tinelli, G. L. Beretta, S. Basili, S. Moro, F. Zunino and A. Battaglia, *J. Med. Chem.*, 2009, **52**, 1029–1039; (g) Y. L. Leu, C. S. Chen, Y. J. Wu and J. W. Chern, *J. Med. Chem.*, 2008, **51**, 1740–1746; (h) Z. Zhang, K. Tanabe, H. Hatta and S. Nishimoto, *Org. Biomol. Chem.*, 2005, **3**, 1905–1910; (i) R. M. Wadkins, D. Bearss, G. Manikumar, M. C. Wani, M. E. Wall and D. D. V. Hoff, *Cancer Res.*, 2004, **64**, 6679–6683; (j) S. Okuno, M. Harada, T. Yano, S. Yano, S. Kiuchi, N. Tsuda, Y. Sakamura, J. Imai, T. Kawaguchi and K. Tsujihara, *Cancer Res.*, 2000, **60**, 2988–2995.
- 23 C. Soldi, A. V. Moro, M. G. Pizzolatti and C. R. D. Correia, *Eur. J. Org. Chem.*, 2012, 3607–3616.
- 24 (a) A. Poli, S. Mongiorgi, L. Cocco and M. Y. Follo, *Biochem. Soc. Trans.*, 2014, **42**, 1471–1476; (b) S. Lim and P. Kaldis, *Development*, 2013, **140**, 3079–3093.
- 25 H. L. Yang, P. J. Huang, S. C. Chen, H. J. Cho, K. J. Kumar, F. J. Lu, C. S. Chen, C. T. Chang and Y. C. Hseu, *Environ. Mol. Mutagen.*, 2014, **55**, 741–750.
- 26 T. G. Cotter, S. V. Lennon, J. G. Glynn and S. J. Martin, *Anti-cancer Res.*, 1990, **10**, 1153–1159.
- 27 C. D. Gregory and J. D. Pound, *J. Pathol.*, 2011, **223**, 178–195.
- 28 S. Fulda and K. M. Debatin, *Oncogene*, 2006, **25**, 4798–4811.
- 29 (a) G. S. Salvesen, *Cell Death Differ.*, 2002, **9**, 3–5; (b) S. Ghavami, M. Hashemi, S. R. Ande, B. Yeganeh, W. Xiao, M. Eshraghi, C. J. Bus, K. Kadkhoda, E. Wiechec, A. J. Halayko and M. Los, *J. Med. Genet.*, 2009, **46**, 497–510.
- 30 H. Zhang, H. L. Xu, W. W. Fu, Y. Xin, M. W. Li, S. J. Wang, X. F. Yu and D. Y. Sui, *Asian Pac. J. Cancer Prev.*, 2014, **15**, 7919–7923.
- 31 (a) G. J. Doherty and H. T. McMahon, *Annu. Rev. Biophys.*, 2008, **37**, 65–95; (b) R. Dominguez and K. C. Holmes, *Annu. Rev. Biophys.*, 2011, **40**, 169–186; (c) S. M. Rafelski and J. A. Theriot, *Annu. Rev. Biochem.*, 2004, **73**, 209–239; (d) C. L. Adams, W. J. Nelson and S. J. Smith, *J. Cell Biol.*, 1996, **135**, 1899–1911.
- 32 (a) Y. Zhang, D. Ouyang, L. Xu, Y. Ji, Q. Zha, J. Cai and X. He, *Acta Biochim. Biophys. Sin.*, 2011, **43**, 556–567; (b) T. D. Pollard and J. A. Cooper, *Science*, 2009, **326**, 1208–1212.
- 33 (a) F. van Zijl, G. Krupitza and W. Mikulits, *Mutat. Res.*, 2011, **728**, 23–34; (b) H. Yamaguchi and J. Condeelis, *Biochim. Biophys. Acta*, 2007, **1773**, 642–652; (c) D. Spano, C. Heck, P. De Antonellis, G. Christofori and M. Zollo, *Semin. Cancer Biol.*, 2012, **22**, 234–249.
- 34 M. Krause, E. W. Dent, J. E. Bear, J. J. Loureiro and F. B. Gertler, *Annu. Rev. Cell Dev. Biol.*, 2003, **19**, 541–564.
- 35 D. Vignjevic and G. Montagnac, *Semin. Cancer Biol.*, 2008, **18**, 12–22.
- 36 P. Zhang, H. R. Hu, Z. H. Huang, J. Y. Lei, Y. Chu and D. Y. Ye, *Bioorg. Med. Chem. Lett.*, 2002, **22**, 7232–7236.
- 37 M. Soda, D. Hu, S. Endo, M. Takemura, J. Li, R. Wada, S. Ifuku, H. T. Zhao, O. El-Kabbani, S. Ohta, K. Yamamura, N. Toyooka, A. Hara and T. Matsunaga, *Eur. J. Med. Chem.*, 2012, **48**, 321–329.